

3

Mixing and mass transfer

3.1 INTRODUCTION

The growth of aerobic organisms in submerged culture is controlled by the availability of substrates, energy, and enzymes. Cultures are always of a heterogeneous nature, and so rates of reactions can be limited by the rate of substrate or product transfer at a particular interface, as shown in Fig. 3.1. Materials might transfer between solid and liquid, gas and liquid, or to the cells. Also, the cells may be aggregated into flocs or even may be immobilized onto some stationary support.

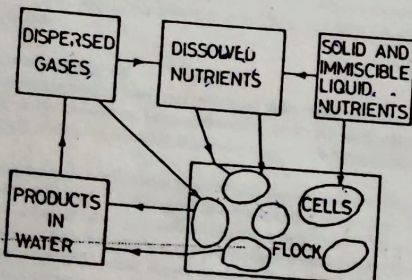


Fig. 3.1 — Material transfer (from European Federation of Biotechnology, (1984) *Process variables in biotechnology*, Dechema).

The transfer of mass is an extremely complex problem. One of the main parameters controlling mass transfer is the degree of agitation, which is also important in maintaining uniform conditions within the bioreactor. In general,

Sec. 3.2]

Mass transfer

89

increased agitation means greater mass transfer; however, it also means a higher power consumption and higher shear. Further, in most systems one mass transfer step is often controlling, and in bioreactors this is often the dissolution of oxygen in water. The rate of oxygen transfer from the gas to the liquid phase will be governed by the size of the air-liquid interface, its resistance to mass transfer, and the hold-up and residence time distribution of air in the vessel; these factors will, in turn, depend on the gas-flowrate and the agitation characteristics (impeller geometry, speed of rotation, power input, etc.) which must be incorporated into the system design.

In this chapter it is proposed to give a basic understanding of the fundamentals of mixing and mass transfer with reference in the main to stirred tank bioreactors, although some discussion of airlift fermenters will be made.

3.2 MASS TRANSFER

3.2.1 Oxygen transfer

The growth of an aerobic organism in submerged culture requires oxygen dissolved in the liquid. Since oxygen is sparingly soluble in aqueous solution, it must be supplied continuously. The transfer of oxygen from the gas to the microorganism takes place in several steps. Firstly, the oxygen must travel through the gas to the gas-liquid interface, then through the interface, through the bulk liquid, and finally into the organism. This entire process is driven by the difference between the oxygen concentration in the gas and in the organism.

It has been found that the rate of oxygen transfer at low concentrations is proportional to the difference in oxygen concentrations. For the transfer to the interface from the bulk liquid this can be written,

$$N_a = k_L (C^* - C_i) \quad (3.1)$$

N_a = Oxygen flux, $\text{kmol}/\text{m}^2\text{s}$

k_L = liquid side mass transfer coefficient, m/s

C^* = oxygen concentration in the liquid at the interface, kmol/m^3

C_i = oxygen concentration in the bulk liquid, kmol/m^3

A gas side mass transfer coefficient can be similarly defined in terms of the gas side partial pressure

$$N_g = K_g (P_g - P_{gi}) \quad (3.2)$$

where K_g = gas side mass transfer coefficient $\text{kmol}/\text{m}^2/\text{bar}$

P_g, P_{gi} = oxygen partial pressure in the gas (bulk and interface respectively), bar

In general it is impossible to measure the interface concentration, so an overall mass transfer coefficient based on the difference in bulk concentrations is used:

Mixing and mass transfer

$$N_a = K_L (C^* - C_L)$$

[Ch. 3]

(3.3)

where K_L = overall mass transfer coefficient based on the difference in equivalent bulk liquid concentrations, m^3/s
 C^* = equivalent liquid concentration in equilibrium with the bulk gas partial pressure, kmol/m^3 .

If Henry's law is obeyed (for small values of C)

$$P = H C^*$$

(3.4)

where H = Henry's law constant

so

$$\frac{1}{k_L} = \frac{1}{H \cdot K_g} + \frac{1}{K_L} \quad (3.5)$$

For slightly soluble gases the rate of diffusion is controlling in the liquid phase, consequently H is large ($4.2 \times 10^4 \text{ bar mol}^{-1}$ fraction for the solution of oxygen in water), so $k_L \approx K_L$.

Since it is usually impossible to determine local concentrations, everywhere in a bioreactor, average values of the concentrations and mass transfer coefficients must be used. To know the total oxygen transfer rate in a vessel, the total surface area available for oxygen transfer has to be determined. This is a difficult quantity to evaluate, so an overall mass transfer coefficient incorporating the surface area of the bubbles is used, namely $K_{L,a}$.

The transfer of oxygen into the bioreactor or the oxygen uptake rate is,

$$N_a = K_{L,a} (C^* - C_L) \quad (3.6)$$

a = surface area of bubbles/unit volume, m^2/m^3

The $K_{L,a}$ value is dependent on the physicochemical properties of the bioreactor media and on the physical properties and operating conditions of the vessel. The magnitude of $K_{L,a}$ can be controlled by the agitation conditions and the air flow rate. Oxygen is a substrate which limits growth; however, above a certain concentration, growth will become independent of oxygen concentration. Knowledge of $K_{L,a}$ behaviour allows the operation of bioreactors at conditions where oxygen is not a limiting factor for growth.

In many cases such as fungi, bacteria, and yeasts this will mean that the agitation is very intense, which in turn will also mean that the shear stresses in the vessel will be large. Plant and animal cells are particularly susceptible to shear, and this has led to different designs of bioreactor other than the conventional stirred tank vessel.

[Ch. 3]

Sec. 3.2]

Mass transfer

91

3.2.2 Measurement of $K_{L,a}$

Methods for measuring $K_{L,a}$ in fermentation processes can be divided into two general types: steady state methods and dynamic methods.

3.2.2.1 Steady state — oxygen balance method

In this method the quantities N_a , C^* , and C_L are measured and then substituted into the equation (3.6) and section 7.4.1 of this volume to find $K_{L,a}$.

$$N_a = K_{L,a} (C^* - C_L)$$

The rate of oxygen transfer, N_a , into the system is obtained by measuring the difference between the amount of oxygen in the streams to and from the bioreactor, and the respective flow rates. As the difference in oxygen concentration between the entrance and exit of the reactor is small, the exit concentration has to be measured very accurately. A mass spectrometer is usually used.

The dissolved oxygen concentration can be measured at one or several points in the vessel (depends on vessel size), using a dissolved oxygen probe. The equilibrium concentration is evaluated from Henry's law.

In large reactors the partial pressure of oxygen in the gas will fall as it passes through the vessel. Therefore a logarithmic mean oxygen concentration of the inlet and outlet gas streams should be used as given below.

$$\log \frac{\text{mean conc}}{\text{Dissolved conc}} = \frac{P_{in} - P_{out}}{\ln(P_{in}/P_{out})} \quad (3.7)$$

and so the equilibrium concentration

$$C^* = \frac{P_{in}}{H} \quad (3.8)$$

This is the most accurate method of measuring $K_{L,a}$, and it can be used on an actual fermentation system; however, it does depend on accurate O₂ analysers which are expensive, and also on accurate measurement of temperature and pressure.

3.2.2.2 Dynamic methods

(a) Static gassing out — This is applicable to a non-respiring system. The oxygen content of the liquid in the bioreactor is reduced to zero by gassing out with nitrogen. The system is then aerated and the value of the dissolved oxygen concentration, C_L , is measured as a function of time. The equation representing this operation is:

$$\frac{dC_L}{dt} = K_{L,a} (C^* - C_L) \quad (3.9)$$

which integrates to (if $C_L = 0$ at time, t_0)

$$\begin{aligned} \left[\ln(C^* - C_L) \right]_{t_0}^t &= K_{L,a} (t - t_0) \\ \ln \left(\frac{C^* - C_L}{C^*} \right) &= K_{L,a} (t - t_0) \end{aligned}$$

Mixing and mass transfer

[Ch. 3]

$$\ln \left(1 - \frac{C_L}{C^*} \right) = -K_{L,a} t \quad (3.10)$$

A graph of $\ln \left(1 - \frac{C_L}{C^*} \right)$ against t will give a straight line of slope $-K_{L,a}$.

The advantage of this method is that it is simple; however, it can, as stated earlier, be used only on a non-respiring system, and it also requires an oxygen probe with a fast response. The method assumes that the oxygen concentration in the gas phase will be the same in both the inlet and outlet streams, which will not be the case, particularly in the initial stages of the re-oxygenation of the liquid. A modified dynamic response technique has been developed by Chapman *et al.* (1982) to overcome this problem.

(b) *Dynamic gassing out* — In this method air supplied to a respiring culture is stopped and the resulting fall in dissolved oxygen concentration is measured. The air supply is switched on before the critical dissolved oxygen concentration is reached, and the increasing dissolved oxygen is recorded as a function of time.

The mass balance of dissolved oxygen in the bioreactor is given by

$$\frac{dC_L}{dt} = K_{L,a}(C^* - C_L) - rX \quad (3.11)$$

where r = specific rate of oxygen uptake by the cell (mol O₂/g cell/l)
 X = cell concentration (g cell/l)

which on rearranging gives,

$$C_L = -\frac{1}{K_{L,a}} \left(rX + \frac{dC_L}{dt} \right) + C^* \quad (3.12)$$

A graph of C_L against $\left(rX + \frac{dC_L}{dt} \right)$ will give a straight line of slope $-\frac{1}{K_{L,a}}$.

This method determines $K_{L,a}$ for an actual fermentation; however, it assumes that the culture is rapidly degassed when the air is stopped, which is not always the case, particularly for a filamentous fungi fermentation broth. The accuracy of the method is also dependent on the dynamic response of the oxygen probe. A modified method taking into account the response of the probe has been developed by Yang *et al.* (1988).

3.2.3 Correlations for $K_{L,a}$ — stirred tanks

Increasing power input reduces bubble size, and so increases interfacial area. Correlations, therefore, for evaluating $K_{L,a}$ as a function of power input/unit volume and also superficial gas velocity, which is the volumetric gas flowrate divided by the cross-sectional area, exist.

Sec. 3.2] Mass transfer

The general form of the correlations for evaluating $K_{L,a}$ is

$$K_{L,a} = x \left(\frac{P_g}{V_L} \right)^y (\nu_g)^z \quad (3.13)$$

where P_g = agitator power under gassing conditions, W
 V_L = liquid volume without gassing, m³
 ν_g = superficial gas velocity, m/s
 $K_{L,a}$ = volumetric mass transfer coefficient, s⁻¹
 x = constant

Many studies of gas-liquid mass transfer in low-viscosity fluids in agitated vessels have been reviewed by Van't Riet (1983). Results of experiments in many different vessels with different agitator configurations all fit within 20–40% of the correlations

(a) For coalescing air-water dispersion

$$K_{L,a} = 2.6 \times 10^{-2} \left(\frac{P_g}{V_L} \right)^{0.4} (\nu_g)^{0.5} \quad (3.14)$$

$$V_L \leq 2.6 \text{ m}^3; 500 < \frac{P_g}{V_L} < 10000.$$

(b) For non-coalescing air-electrolyte dispersion

$$K_{L,a} = 2 \times 10^{-3} \left(\frac{P_g}{V_L} \right)^{0.7} (\nu_g)^{0.5} \quad (3.15)$$

$$V_L \leq 4 \text{ m}^3; 500 < \frac{P_g}{V_L} < 10000.$$

In general, coalescing systems are ones where the water is relatively pure and non-coalescing systems are ones where a small amount of electrolyte is in the system. These correlations do not take into account the non-Newtonian behaviour of biological fluids, nor the effect of antifoam and the presence of solids. A correlation that has been shown to apply to a non-Newtonian filamentous fermentation is of the form:

$$K_{L,a} = x \left(\frac{P_g}{V_L} \right)^{0.33} (\nu_g)^{0.54} \quad (3.16)$$

Comparing this with the equation for Newtonian fluids shows that the oxygen transfer coefficient for non-Newtonian fluids is less sensitive to increases in power input, so more power is required to reach the same $K_{L\alpha}$ value than in a Newtonian fluid.

The addition of antifoam has a significant effect on the $K_{L\alpha}$ value. The effect of the antifoam is to reduce the interfacial free energy at the phase interface between the water and air, so reducing surface tension and decreasing the bubble diameter, leading to higher values of the interfacial area per unit volume, a . However, the tendency for a to increase is countered by the effect of the surfactant film on the mass transfer coefficient K_L . This decrease may be due to either or both of the following mechanisms: the liquid movement near the interface is reduced because of the decreased mobility of the interface, and the increased resistance of the molecular film results in a different vapour/liquid equilibrium at the interface.

In general, with modern silicon-based antifoams, the decrease in K_L seems to be larger than the increase in a , which means the overall $K_{L\alpha}$ value is reduced at all concentrations. However, with other surfactants (sodium dodecyl sulphate and sodium lauryl sulphate) it has been shown that the $K_{L\alpha}$ value increased with increasing concentration.

3.2.4 Correlations for $K_{L\alpha}$ — airlift bioreactors

There are a wide range of correlations dependent on the configurations of the bioreactor, that is, whether there is an internal draught tube or an external loop, whether the draught tube or the annulus is sparged.

A typical correlation for a wide range of configurations is

$$K_{L\alpha} = 5.5 \times 10^{-4} \left(1 + \frac{A_d}{A_r}\right)^{-1.2} \left(\frac{P_g}{V_L}\right)^{0.8}, \quad (3.17)$$

or in terms of the superficial gas velocity in the riser v_{gr} , m/s

$$K_{L\alpha} = 0.76 \left[1 + \frac{A_d}{A_r}\right]^{-2} v_{gr}^{0.8}, \quad (3.18)$$

where A_d = downcomer cross-sectional area, m^2

A_r = riser cross-sectional area, m^2

v_{gr} = superficial gas velocity in the riser, $m.s^{-1}$.

The correlation has been tested in various bioreactors at differing air flow rates, and the results are shown in Fig. 3.2. It can be seen that agreement was within 20% of the measured values; however, in a real system with antifoam and dispersed solids, the results could be different. The aspect ratio of the fermenters used was 5 to 1 (10 litres), 12 to 1 (30 litres), 6.5 to 1 (100 litres), and 8.5 to 1 (1000 litres).

A more detailed review of correlations to evaluate $K_{L\alpha}$ is given by Chisti (1989a,b).

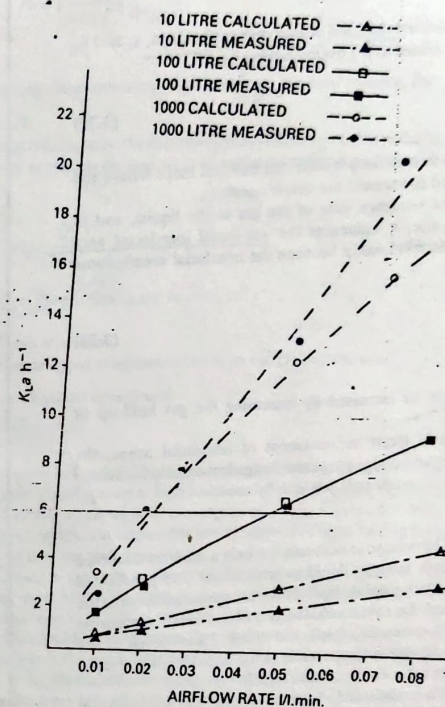


Fig. 3.2 — The effect of air flow rate on oxygen transfer coefficients, $K_{L\alpha}$ (from Wood, L. A. & Thompson, P. W. (1986).

3.2.5 Gas hold-up

The volume fraction of gas-phase in the gas-liquid dispersion is known as the gas hold-up or the gas void fraction. The overall gas hold-up (ϵ) is given by

$$\epsilon = \frac{V_g}{V_g + V_L} \quad (3.19)$$

where V_g and V_L are the gas and liquid volumes in the reactor.

Mixing and mass transfer

[Ch. 3]

In airlift bioreactors the individual riser and downcomer gas holdups, ϵ_r and ϵ_d can be evaluated and these are related to the overall holdup by

$$\epsilon = \frac{A_r \epsilon_r + A_d \epsilon_d}{A_r + A_d} \quad (3.20)$$

This equation is valid for both internal-loop airlifts and external loops where the dispersion height in the riser and downcomer are nearly equal.

Gas hold-up determines the residence time of the gas in the liquid, and in combination with the bubble size, it influences the gas-liquid interfacial area available for mass transfer. The relationship between the interfacial area/volume reactor and hold-up is given by

$$a = \frac{6\epsilon}{d} \quad (3.21)$$

where d = bubble diameter.

So, the interfacial area may be increased by increasing the gas hold-up or decreasing the bubble size.

Because of the difficulties in direct measurement of interfacial areas, the parameter is little used for bioreactor design purposes. Instead, the easily measured overall volumetric mass transfer coefficient $K_{L,a}$ is usually used.

3.2.6 Liquid mixing

Efficient liquid is essential in a bioreactor to maintain not only a uniform dissolved oxygen concentration, but also a uniform liquid concentration. The concept of mixing time can be introduced, which is defined as the time for a point addition to the vessel being uniformly distributed. There are a wide variety of methods of measuring mixing time (Edwards 1985). However, in a gas/liquid system, knowledge of the value of the mixing time is usually not too important, as the liquid mixing is rapid compared with the mass transfer between the air and liquid.

It has been shown that there is a relationship between mixing time and gas hold-up, ϵ (Middleton 1985). At gas hold-up values of 0.1 (a typical value for an aqueous solution) mixing time is changed only slightly by the presence of gas; however, at values of approximately 0.2, mixing time is increased. At much higher gas hold-ups > 0.7 (unlikely to be required in bioreactor systems) liquid is mostly in the form of films between bubbles with restricted mobility, so poor mixing occurs.

3.3 THEORY OF MIXING

The object of mixing in a gas/liquid/solid system are to:

- Create small bubbles and so increase the interfacial area.
- Disperse the bubbles throughout the liquid.
- Keep the bubbles in the liquid by recirculation for a sufficient time.

Sec. 3.3]

Theory of mixing

- Maintain uniform conditions in the vessel and provide turbulent eddies to feed liquid to and from the interfaces.
- Maintain the solid in suspension and in particular prevent sedimentation on the bottom of the vessel.
- Maintain a uniform temperature in the vessel.

High-energy turbulence is required for (a) and high flow for (b-f).

The following treatment of mixing refers only to stirred-tank vessels, as airlift bioreactors are considered in Chapter 5.

3.3.1 Characterization of agitation

The following treatment of agitation is restricted to fluids that approximate to Newtonian liquids.

As mixing is extremely complex, the variables involved are lumped together into dimensionless groups to obtain correlations that describe the system. The Reynolds number is used to characterize the flow

$$Re = \frac{D_i^2 N \rho}{\mu} \quad (3.22)$$

where D_i = impeller diameter, m

N = impeller speed, Hz

ρ = fluid density, kg/m³

μ = fluid viscosity, kg/m.s.

Fully turbulent flow exists above a Reynolds number of 10^4 , while fully laminar flow exists below 100, and in between is the transition region. Another group which is used to characterize mixing in a vessel which takes into account gravitational effects is the Froude number,

$$Fr = \frac{N^2 D_i}{g} \quad (3.23)$$

where g = gravitational acceleration, m/s²

A third group which relates to the energy required by the agitator is the power number

$$P_a = \frac{P}{N^3 D_i^5 \rho} \quad (3.24)$$

where P = agitator power, W

The power number has been correlated with Reynolds number for several types of agitators, as shown in Fig. 3.3 for Newtonian liquids with no aeration. The power refers to the shaft power, and so allowances must be made for electrical and friction losses when calculating motor power input.

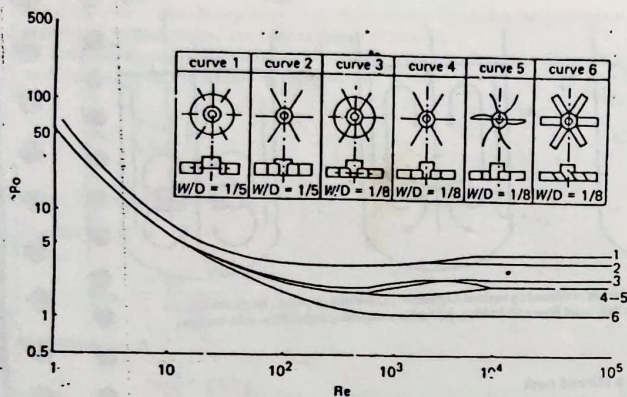


Fig. 3.3 The variation of power number (P_o) with Reynolds number (Re) with various impellers (from Uhl. V. W. & Gray, J. B. 1966).

In general, the laminar region, where K_1 is a constant

$$P_o = K_1 Re^{-1}, \quad K_1 \propto \frac{1}{\rho e} \quad (3.25)$$

and in the turbulent region the power number is independent of the Reynolds number. Under these conditions

$$P_o = K_2 N^3 D_i^3 \rho, \quad (3.26)$$

and the power is independent of the viscosity.

It is also useful to define another number which relates to the flow rate generated by the impeller. The action of an agitator blade can be likened to a casedless pump. The power input can be written as,

$$P = \rho Q g H' \quad (3.27)$$

where Q = flow rate created by the impeller

H' = the head which is dissipated on circulation through the vessel.

With low-viscosity fluids, the head is equivalent to the turbulence generated, which is most intense in the region of the impeller and decreases considerably in the outer areas of the vessel.

Substituting the power term into the expression for the power number,

$$P_o = \left(\frac{Q}{ND_i^3} \right) \left(\frac{gH'}{N^2 D_i^2} \right). \quad (3.28)$$

The resulting dimensionless groups are $\frac{gH'}{N^2 D_i^2}$, the head number, and $\frac{Q}{ND_i^3}$, the flow number, Fl .

In an aerated system, the effective density of the mixture is reduced, which affects the power requirement, and so it is useful to define a modified flow number as follows,

$$Fl_g = \frac{Q_g}{ND_i^3} \quad (3.29)$$

Where Q_g is the gas flow in the reactor, $m^3 s^{-1}$.

3.3.2 Types of agitator

Three common types of agitator have been used in bioreactors:

- Turbine (Rushton or inclined)
- Propeller
- INTERMIG*

They are shown in Fig. 3.4. These types of agitator are used in low-viscosity systems $\mu < 50 \text{ kg m s}^{-1}$ and operate at high rotational speeds. A typical tip speed for turbine and INTERMIG agitators is in the region of 3 m/s, a propeller being somewhat faster. These impellers are classed as remote clearance types having diameters in the range 25–66% of the tank diameter.

The turbine is the most common of the three types of agitator. It consists of a number of short blades attached to a central shaft. The diameter of a turbine is normally between 30 to 50% of the tank diameter, and there are usually 4–6 blades. Turbines with flat blades give radial flow as shown in Fig. 3.5, which is good for gas dispersion where the gas is introduced just below the impeller on the axis and is drawn up to the blades and broken up into fine bubbles.

Where solids are present as in a fermentation, it is found that an axial component is useful to keep the solids in suspension, and a pitch turbine with a back angle of 45° is used.

The propeller agitator usually has three blades and revolves at relatively high speeds, 60–300 Hz, to obtain efficient mixing. The flow pattern generated, shown in Fig. 3.5, is called axial flow since the fluid flows axially down the centre axis and up on the sides of the tank.

Recent developments in agitator design have led to the INTERMIG agitator. This is an axial pumping impeller in which blades are angled such that they oppose each other. This results in a more uniform transfer of energy throughout the vessel compared with a disk turbine. This type of agitator requires 25% less power to obtain the same degree of mixing and reduced air throughput to obtain the same $K_1 a$ value.

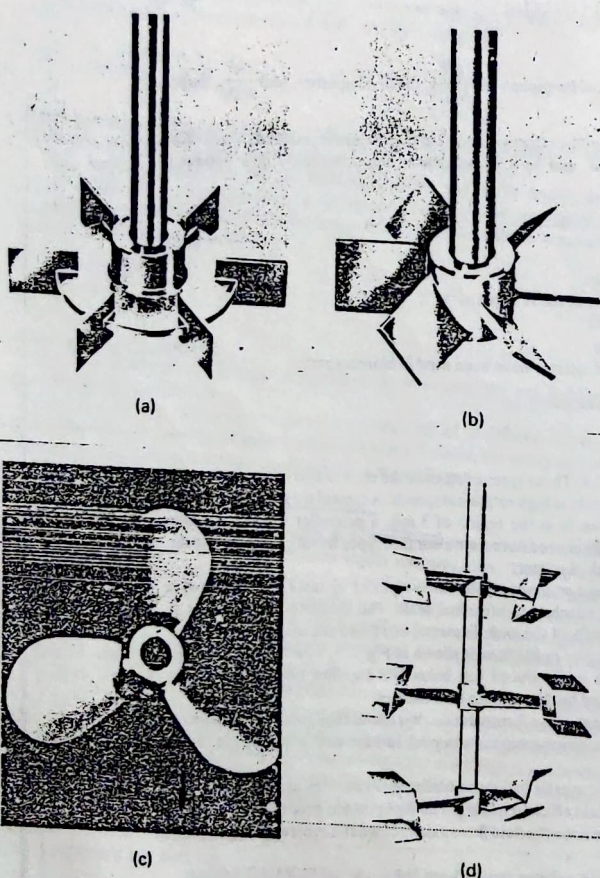


Fig. 3.4 — Four common types of impeller. (a) Rushton turbine, (b) inclined turbine, (c) propeller, (d) INTERMIG.

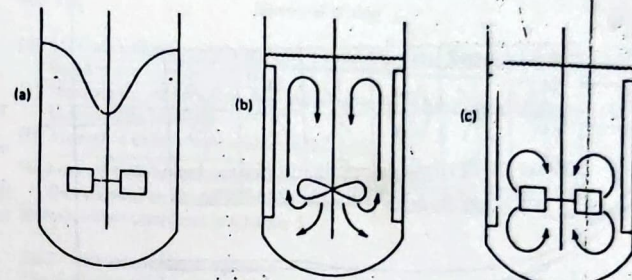


Fig. 3.5 — Flow patterns produced by various impellers. (a) turbine impeller, large vortex, no baffles, (b) propeller, axial flow with baffles, (c) turbine impeller, radial flow with baffles.

3.3.3 Agitation in a stirred tank

There are more data available on turbine agitators than on any of the other agitators mentioned, so the discussion below concentrates on turbines. If a gas-liquid two-phase system is considered, the effect of the flow regimes on increasing agitation can be seen in Fig. 3.6 (Nienow *et al.* 1985). With a low agitator speed, the flow pattern is

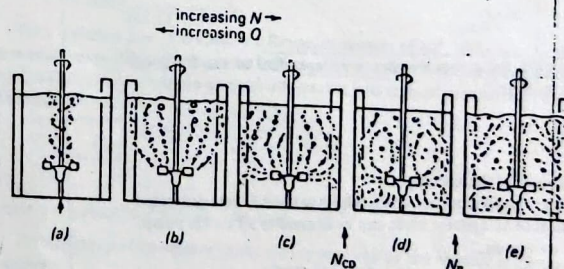


Fig. 3.6 — Flow regimes in a stirred-tank bioreactor with increasing impeller speeds (N), and increasing flow rate produced by the impeller (Q). N_{CD} is the impeller speed below which the gas does not penetrate below the impeller, and N_R is the impeller speed at which gross recirculation of gas back into the agitator occurs (from Nienow *et al.* 1985).

dominated by the gas-liquid flow up the middle, that is, the impeller is said to be flooded. Increasing the speed creates a flow pattern dominated by the agitator in which the flow is horizontally dispersed from the agitator, and then above a certain

speed, the flow is distributed to all parts of the vessel. Increasing the gassing rate Q_g at constant N leads to the opposite sequence of events.

The flooding point N_F and the point at which complete dispersion occurs N_{CD} can be calculated from the following correlations:

$$N_F = \left(\frac{Q_g T}{3D_i^2} \right) \quad (3.30)$$

where T = vessel diameter, m.

For pipe spargers

$$N_{CD} = \frac{(4Q_g^{0.5} T^{0.25})}{D_i^2} \quad (3.31)$$

For ring spargers

$$N_{CD} = \frac{(3Q_g^{0.5} T^{0.25})}{D_i^2} \quad (3.32)$$

The speed N_{CD} is important as it gives the speed below which the gas does not penetrate beneath the agitator and the whole tank is not used. A further critical speed can also be calculated, N_R , which is the speed which gross recirculation of gas back into the agitator occurs.

N_R is given by

$$N_R = \frac{(1.5Q_g^{0.2} T)}{D_i^2} \quad (3.33)$$

These correlation are in SI units and are valid for coalescing systems in tanks up to 1.8 m diameter, with a 6-bladed disk turbine, where $h = T$, and $C_l = 7/4$

where h = height of tank

C_l = clearance of impeller above the bottom of the tank.

3.3.4 Effect of gas and solids on power consumption

Knowledge of the power, P_g , absorbed by the system is required for the determination of mass transfer rates, gas hold-up, and interfacial area on the large scale from small-scale tests. The ungassed power consumption can be calculated from the power number, see Fig. 3.3. When gas is sparged into the system at a given speed, the power decreases, as shown in Fig. 3.7, because of the formation of gas cavities behind the blades.

The gassed power consumption can be evaluated from the following equation obtained by Michel & Müller (1962).

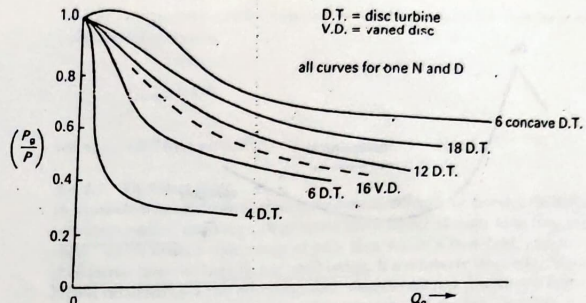


Fig. 3.7 — Agitator power curves for various impellers with increasing gas flow (Q_g). P_g : agitator power under gassing; P : agitator power without gassing; D. T.: disk turbine with 4–18 vanes; V. D.: vaned disk (from Middleton, J. C. (1985)).

$$P_g = 0.706 \left(\frac{P^2 N D_i^3}{Q_g^{0.56}} \right)^{0.45} \quad (3.34)$$

If a plot of P_g against Q_g is made as shown in Fig. 3.8 at constant Q_g and increasing N , then a minimum is found at N_{CD} . The explanation of the shape of the curve (Middleton 1985) is that in the region at the lowest speed, the gas passes mainly through the agitator without dispersion and the liquid flows around the outer part of the blades undisturbed by the gas. Therefore, the gassed power is not much different to the single phase liquid system. As N increases, gas is captured by the vortices behind the agitator blades, and dispersed and so P_g decreases as the captured gas 'streamlines' the blades forming large cavities. Further increase of N diminishes the cavities which allows the air to be dispersed and results in larger values of P_g . The power continues its rise with increasing speed until N_R is reached at which gross circulation of gas back into the agitator arises.

The previous discussion refers to a system where solid is not present. In bioreactors containing cultures, the system becomes three-phase and so more complex. It is important to prevent the solid settling on the bottom of the vessel and to keep an even distribution. It has been found that the clearance of the agitator above the base of the vessel is important, and that an optimum is reached when this distance is $\frac{1}{2}$ of the tank diameter.

There are considerable advantages in using angled blade agitators for three-phase systems, in that less power is required and greater stability may be achieved. Also, the maximum shear will be reduced. However, the interactions with the sparger are more complex than with disk turbines, and more work is necessary to

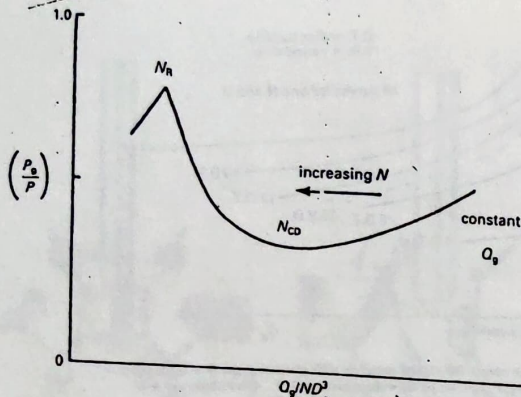


Fig. 3.8 — Agitator power curve at a constant gassing rate (Q_g). P_g , agitator power under gassing; P , agitator power without gassing; Q_g/ND^2 = modified flow number H_g , where Q_g , gas does not penetrate below the impeller; N_R , the impeller speed below which the of gas back into the impeller occurs (from Middleton, J. C. (1985)).

determine optimum geometries. Inclined blade agitators are extremely sensitive to aeration rates at D_f/T ratios of 0.33 or less, which leads to poor suspension. At values of D_f/T of between 0.4 and 0.5, these instabilities disappear and particle suspension efficiency is satisfactory.

3.4 RHEOLOGICAL PROPERTIES

The rheological properties of the media in the bioreactor will affect the power consumption and, therefore, the heat and mass transfer rates. These properties can also change markedly as the biomass in a reactor increases. An example is the production of antibiotics by filamentous organisms. There is also a relationship between shear and rheological properties. Plant and animal cells are exceedingly susceptible to shear damage, which consequently requires a modified reactor design to limit shear (van Wezel & van der Velde-de-Groot 1978).

3.4.1 Rheological classification

Fluids normally encountered in bioreactors can be defined as Newtonian or non-Newtonian. The rheological characteristics of these fluids can be described by the following general equation:

$$\tau = \tau_0 + k(\gamma)^n$$

(3.35)

Sec. 3.4]

Rheological properties

- where τ = shear stress, N/m^2
 τ_0 = yield stress, N/m^2
 γ = shear rate, s^{-1}
 k = consistency index.
 n = flow behaviour index.

The shear rate γ is the velocity gradient and can be written for the case of laminar flow in the x direction as dv/dy where v is the velocity and y is the distance perpendicular to the x direction.

3.4.1.1 Newtonian fluids $n=1$: $\rho_s \approx 0$

These exhibit no yield stress, so $n=1$, $\tau_0=0$, and k becomes μ , the dynamic viscosity, so,

$$\tau = \mu \gamma$$

(3.36)

Newtonian fluids have a viscosity which is independent of shear rate. A number of bacterial and yeast fermentation fluids exhibit Newtonian behaviour.

3.4.1.2 Non-Newtonian fluids

(a) Pseudoplastics

These fluids follow a power law model

$$\tau = k(\gamma)^n$$

(3.37)

where k and n change during the course of the fermentation and will decrease with increasing shear rate.

The apparent viscosity can be defined by the equation

$$\mu_{app} = \frac{\tau}{\gamma} = k\gamma^{n-1}$$

(3.38)

Many filamentous organisms exhibit this characteristic.

(b) Dilatants $n > 1$

These fluids also obey the power law model, but in this case $n > 1$.

(c) Bingham plastics and Casson fluids

These fluids are characterized by the relatively high yield stress required to make the fluids flow. Very few organisms grown in bioreactors exhibit this behaviour.

The rheological characteristics of all these different fluids are shown on the shear-stress diagram, Fig. 3.9.

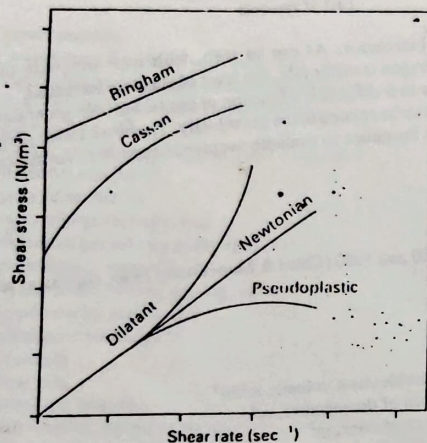


Fig. 3.9 -- Rheological characteristics of fluids

3.4.2 Shear in stirred-tank bioreactors

In a stirred-tank bioreactor, the Reynolds Number of the bulk flow is given by

$$Re = \frac{ND_i^2\rho}{\mu} \quad (3.21)$$

If this impeller Reynolds number exceeds approximately 1000, the flow becomes completely turbulent. To maintain uniform conditions and to ensure complete suspension of the microorganism, most stirred-tank vessels operate in the turbulent regime.

In a turbulent flow field, there are both time-average and time-fluctuating components. If the fluctuating velocity changes rapidly with time or position, strong hydrodynamic forces are created which can damage cells. Strong forces can also be created if the time-average components change greatly over small intervals in position. Both of these types of force need to be considered when evaluating shear.

3.4.2.1 Time-average shear or laminar shear

The maximum time-average shear rate is proportional to the top speed of the impeller, and is given by $\gamma_{max} = KND_i$.

Analysing flow profiles of Croughan *et al.* (1987), showed that $K = 1.26 \text{ cm}^{-1}$.

The average shear rate for an unbaffled vessel under turbulent flow for geometrically similar systems is:

$$\bar{\gamma}_{average} = k_1 N \quad (3.40)$$

where $k_1 = 0.7$ for a ratio T/D_i of 2.

3.4.2.2 Turbulent shear

In a turbulent flow field short-term hydrodynamic forces arise through the motion of turbulent eddies, and they can generate much higher stresses than time-average shear. There exists a wide range of eddy sizes within a flow field, and energy is transferred from the large to the small eddies. If a relatively large eddy forms in a region occupied by a cell microorganism, then the microorganism will rotate and translate in a manner that will reduce the net forces on its surface. However, if a very small eddy of comparable size to or smaller than the microorganism forms adjacent to the cell, then the cell will experience the full force of the eddy. As plant and animal cells are large, they are more susceptible to turbulent shear. In a comprehensive review, Croughan *et al.* (1987) investigated the effect of shear on animal cells in microcarrier cultures. Detrimental effects were apparent when the eddy size was below 100 μm (measured by the Kolmogorov scale L), which was about half the size of the average microcarrier diameter.

The eddy length (Davis 1972),

$$L = \left[\left(\frac{\mu}{\rho} \right)^3 / \rho \right]^{1/4} \quad (3.41)$$

where ρ = power dissipation/unit mass.

Shear damage to other cells has been investigated by several workers (Midler & Finn 1966, Tanaka *et al.* 1975a,b, Taguchi *et al.* 1968). In general, they showed that shear damage was related to the time-average shear (that is $\propto ND_i$).

One of the main problems with most of this work is that it was done on tanks of only a few litres capacity, and there are no data relating to scale-up. Industrial experience has indicated that the dependence on tip speed does not hold over large-scale changes. Part of the reason for this may be that on the industrial scale, agitators work under fully turbulent conditions, whereas this may not be the case on a laboratory scale. For example, compare a 10 m³ vessel with a 1 m diameter impeller running at 1.7 Hz with a 110 l tank which has a 0.1 m impeller running at 17 Hz. Both have a tip speed of 5.2 m s⁻¹. Suppose that the broth has a viscosity of 0.1 N s m⁻² (100 cP) at 18.3 s⁻¹, which is a typical shear rate in the large tank. These values result in a value for the Reynolds number in the large tank of 1.7×10^4 ; however, in the small vessel the value is 1.7×10^3 , which means that the flow is approaching the laminar regime and so the maximum shear will be lower.

4.3 Shear in airlift bioreactors

In an airlift bioreactor, the stresses generated are less than in a stirred-tank bioreactor because the intensity of turbulence is much lower. Time-average or laminar shear values will give the maximum shear values attained in the vessel.

The maximum shear rate will occur at the vessel wall, and the Biaxius equation can be used to evaluate the shear stress where,

$$\frac{\tau}{\rho v_{LR}^2} = 0.0396 Re^{-0.25} \quad (3.42)$$

where $2500 < Re < 100000$ and v_{LR} = liquid velocity in the riser.

The shear rate can be calculated from the standard relationship $\tau = \mu\gamma$ (3.36), for Newtonian fluids and the power law relationship $\tau = Ky^\alpha$ (3.37) for non-Newtonian fluids.

The liquid circulation velocity is a function of the power input to the bioreactor, which is also related to the overall mass transfer coefficient, $K_1 a$. Therefore, it is possible to evaluate the maximum achievable oxygen transfer rate if the maximum permissible shear stress is known. Fig. 3.10 (Wood & Thompson 1986) shows results

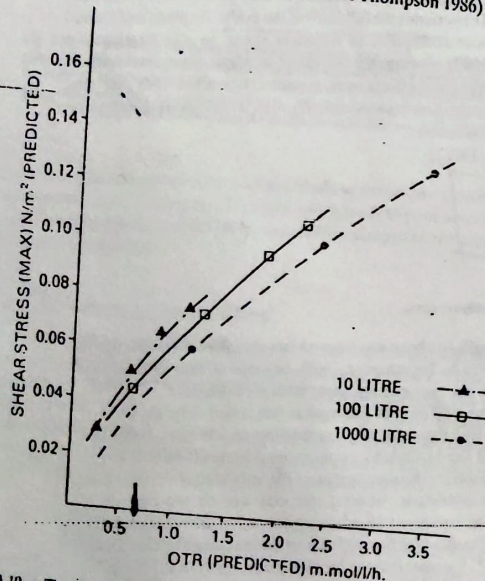


Fig. 3.10 — The relationship between predicted oxygen transfer rate (OTR) and predicted shear stress (N/m^2) in 3 sizes of airlift bioreactor (from Wood, L. A. & Thompson, P. W. 1986).

Sec. 3.5]

List of symbols

109

for three sizes of airlift bioreactor. As can be seen, with increasing size of the bioreactor for the same oxygen transfer rate, the level of shear is decreased.

The average shear rate in a column is a function of the turbulence generated by the rising gas bubbles and can be related to the gas velocity. There are a wide range of correlations quoted in the literature to evaluate average shear rates, the majority, however, are of the form

$$\gamma = kv_{gr} \quad (3.43)$$

where k varies between 1500 and 5000 (Chisti & Moo-Young 1980, Nishikawa *et al.* 1977).

3.5 LIST OF SYMBOLS

a	surface area of bubbles/unit volume, m^2/m^3
A_d	cross-sectional area of downcomer, m^2
A_r	cross-sectional area of riser, m^2
C	partial pressure, $Kmol/m^3$
C_l	clearance of impeller above bottom of tank, m
C^*	oxygen concentration in the bulk liquid, $kmol/m^3$
C_i	oxygen concentration in the liquid at the interface, $kmol/m^3$
D_i	equivalent liquid concentration in equilibrium with the bulk gas $kmol/m^3$
d	impeller diameter, m
H	bubble diameter, m
F_l	flow number
F_{lg}	flow number gassed
Fr	Froude number
g	gravitational acceleration, m/s^2
H	Henry's law constant bar/mol
H'	height of tank, m
h	heads, m
K_L	liquid side mass transfer coefficient, m/s
$K_1 a$	overall mass transfer coefficient, h^{-1}
K_g	gas side mass transfer coefficient, $kmol/m^2 \cdot s / bar$
L	eddy length μm
N_a	oxygen flux, $kmol/m^2 \cdot s$
N	impeller speed, Hz
N_{CD}	complete dispersion speed, Hz
N_f	impeller flooding point
N_R	impeller speed producing recirculation of gas, Hz
OTR	oxygen transfer rate ($g/l/h$)
P	agitator power, W
P_g	oxygen partial pressure in gas, bulk, bar
	agitator power under gassing, W

P_o	power number
P_m	oxygen partial pressure in gas interface, bar
P_{LM}	logarithmic mean oxygen concentration of inlet and outlet gas bar
Q	flow rate produced by the impeller m ³ /s
Q_s	gas flow rate, m ³ /s
r	specific rate of oxygen uptake, mol O ₂ /g cell/s
Re	Reynolds number
T	vessel diameter, m
v_s	superficial gas velocity, m/s
v_p	superficial gas velocity in the riser, m/s
V_x	gas volume in reactor m ³
V_L	liquid volume without gassing, m ³
V_{LR}	liquid velocity in riser, m/s
X	cell concentration, g l ⁻¹
x	a constant
γ	shear rate, s ⁻¹
c	overall gas hold-up
μ	fluid viscosity, kg/m/s or Ns/m ²
μ_{app}	apparent viscosity, kg/m/s
ρ	fluid density, kg/m ³
τ	shear stress, N/m ²
τ_0	yield stress, N/m ²

REFERENCES

- Chapman, C. M., Gibiloro, L. G., & Nienow, A. W. (1982). A dynamic response technique for the estimation of gas-liquid mass transfer coefficients in a stirred vessel. *Chem. Eng. Sci.*, **37**, 891-900.
- Chisti, M. Y. (1989a). Airlift bioreactors. Elsevier Applied Sciences, Amsterdam.
- Chisti, M. Y. (1989b). Airlift reactors. Design and diversity. *The Chemical Engineer*, **457**, 41-45.
- Chisti, M. Y. & Moo-Young, M. (1980). The calculations of shear rate and apparent viscosity in airlift and bubble column bioreactors. *Biotec. Bioeng.*, **34**, 1391-1400.
- Croughan, M. S., Hamel, J. F., & Wang, D. I. C. (1987). Hydrodynamic effects on animal cells grown in microcarrier cultures. *Biotec. Bioeng.*, **29**, 130-135.
- Davis, J. T. (1972). *Turbulence phenomena*. Academic Press, London.
- Edwards, M. F. (1985). Mixing of low-viscosity liquids in stirred tanks. In: Harnby, N., Edwards, M. F. & Nienow, A. W. (eds.) *Mixing in the process industries*. Butterworth Press, Stoneham, 140-145. European Federation of Biotechnology (1984) *Process variables in biotechnology*. Dechema, Frankfurt.
- Michel, B. J. & Miller, S. A. (1962). Power requirements of gas-liquid agitated systems. *A. I. Ch. E. J.*, **8**, 262-265.
- Middleton, J. C. (1985). Gas-liquid dispersion and mixing. In: Harnby, N., Edwards, M. F. & Nienow, A. W. (eds.) *Mixing in the process industries*. Butterworth Press, Stoneham, pp. 337-345.

- Midler, M. & Finn, R. K. (1966). A model system for evaluating shear in the design of stirred fermenters. *Biotec. Bioeng.*, **8**, 71-80.
- Nienow, A., Konno, M., & Buijski, W. (1985). Studies on three-phase mixing. A review and recent results. In: *Proceedings of 5th European Conference on Mixing*, Wurzburg. BHRA, Cranfield, 1-13.
- Nishikawa, M., Kato, H., & Hashimoto, K. (1977). Heat transfer in aerated towers filled with non-Newtonian fluids. *Ind. Eng. Chem. Proc. Design Develop.*, **16**, 133-135.
- Taguchi, H., Imanaka, S., Teramoto, S., Takatake, M., & Satu, M. (1968). Scale-up of glucoamylase fermentation by *Endomyces* sp. *J. Ferment. Technol.*, **46**, 814-816.
- Tanaka, H., Mizugushi, T., & Ueda, J. (1975a). Leakage of intracellular nucleotides in aeration-agitation cultures of mold and identification of the nucleotides. *J. Ferment. Technol.*, **53**, 18-21.
- Tanaka, H., Mizugushi, T., & Ueda, K. (1975b). An index representing the mycelial strength to maintain physiological activity on mechanical agitation. *J. Ferment. Technol.*, **53**, 35-38.
- Uhl, V. W. & Gray, J. B. (1966). *Mixing theory and practice*. Academic Press, London.
- Van't Riet, K. (1983). Mass transfer in fermentation. *Trends in Biotec.*, **1**, 113-115.
- van Wezel, A. & van der Velden-de Groot, C. (1978). Large scale cultivation of animal cells in microcarrier culture. *Proc. Biochem.*, **13**, 6-9.
- Wood, L. A. & Thompson, P. W. (1986). Applications of airlift fermenters. In: Wood, L. A. & Thompson, P. W. (eds.) *Proceedings of Int. Conference on Bioreactor Fluid Dynamics*, Cambridge, 1986. BHRA, Cranfield, 157-166.
- Yang, X. M., Mao, Z. X., Yang, S. Z. & Mao, M. Y. (1988). An improved method for determination of the volumetric oxygen transfer coefficient in fermentation processes. *Biotec. Bioeng.*, **31**, 1006-1009.